A Journal of the Gesellschaft Deutscher Chemiker

Angewandte International Edition Chemie

www.angewandte.org

2017–56/27

Adjusting adsorption selectivity ...

… and separation in photochromic metal–organic frameworks (MOFs) just by external stimuli is highly important but still rare. In their Communication on page 7900 ff., F. Luo, G.-C. Guo, and co-workers employ a photochromic diarylethene unit as a light-triggered selectivity and separation regulator, leading to ultrahigh adsorption selectivity, for example, for the mixture C_2H_2/C_2H_4.

150 Years GDCh

WILEY-VCH

Photochromism

International Edition: DOI: 10.1002/anie.201702484
German Edition: DOI: 10.1002/ange.201702484

Significant Enhancement of C_2H_2/C_2H_4 Separation by a Photochromic Diarylethene Unit: A Temperature- and Light-Responsive Separation Switch

Cong Bin Fan[+], Le Le Gong[+], Ling Huang[+], Feng Luo, Rajamani Krishna,* Xian Feng Yi, An Min Zheng,* Le Zhang, Shou Zhi Pu,* Xue Feng Feng, Ming Biao Luo, and Guo Cong Guo**

Abstract: *A dual temperature- and light-responsive C_2H_2/C_2H_4 separation switch in a diarylethene metal–organic framework (MOF) is presented. At 195 K and 100 kPa this MOF shows ultrahigh C_2H_2/C_2H_4 selectivity of 47.1, which is almost 21.4 times larger than the corresponding value of 2.2 at 293 K and 100 kPa, or 15.7 times larger than the value of 3.0 for the material under UV at 195 K and 100 kPa. The origin of this unique control in C_2H_2/C_2H_4 selectivity, as unveiled by density functional calculations, is due to a guest discriminatory gate-opening effect from the diarylethene unit.*

Metal–organic frameworks (MOFs) have been recently intensively researched, consequently leading to many applications, including, but not limited to, luminescence, sensors, catalysis, storage, and separation.[1–5] In particular, and as an improvement over traditional zeolites and porous carbon, MOFs are now used to enable excellent CO_2/N_2, CO_2/CH_4, and CO_2/H_2 separation.[6,7] However, for some important applications, such as that of C_2H_2/CO_2 and C_2H_2/C_2H_4 separation, because of their comparable size and physical nature, most MOFs exhibit only modest separation.[8,9]

An ideal separation material is viewed to endow both high selectivity and adsorption capacity.[1b] However, almost all reported MOFs encounter a so-called trade-off, namely high selectivity often resulting in low adsorption capacity, and vice versa.[1b] To address this issue, one possible method is to anchor exclusive functional site for special guest molecule, but without sacrificing adsorption capacity, leading to enhanced adsorption selectivity. MOF-74 presents a good example of using open metal site to preferentially adsorb CO_2 over N_2 and CH_4.[10] UTSA-74, a MOF-74 isomer, is observed to give excellent C_2H_2/CO_2 selectivity and separation, owing to its unique open metal site of two accessible gas binding sites per metal ion.[11] In some cases, decorating organic ligands with functionalized units such as NH_2 or amide is also used to enhance adsorption selectivity.[12] Another interesting case reported by Kitagawa et al. is based on two ideally arranged basic oxygen atoms on the pore wall that preferentially adsorbs C_2H_2 adsorption over CO_2, because of the difference in acidity of the hydrogen atoms.[13] Moreover, a guest discriminatory gate effect observed in a flexible MOFs is used to generate inverse CO_2/C_2H_2 selectivity.[14] Very recently, control in both pore and size by Chen et al. was employed to generate an ultrahigh C_2H_2/C_2H_4 selectivity of 44.8.[15]

In contrast to the above mentioned strategies that demand precise MOF design,[11–15] the approach followed in the current work is to utilize external stimuli (for example, heat, light, magnetic) to modulate adsorption selectivity; this is demonstrated to be easy to implement. Such a smart material can be constructed with some specific elements on MOFs that are responsive to external stimuli, and accordingly shows dynamical alteration in their physical properties.[16–19] In view of this, controlling CO_2 uptake in MOFs has been achieved by heat, or light, or a magnet.[20] However, until now no case of using external stimulus to modulate adsorption selectivity in MOFs has been reported.

Diarylethene, which not only undergoes a fast, reversible photoinduced ring-open to ring-closed transformation, but also affords high photostability for each isomer, has been

[*] L. L. Gong,[+] Prof. Dr. F. Luo, L. Zhang, X. F. Feng, M. B. Luo
School of Biology, Chemistry and Material Science, East China University of Technology
NanChang, Jiangxi 344000 (China)
E-mail: ecitluofeng@163.com
Prof. Dr. G. C. Guo
State Key Laboratory of Structural Chemistry, Fujian Institute of Research on the Structure of Matter, Chinese Academy of Sciences
Fuzhou
Fujian 350002 (China)
E-mail: gcguo@fjirsm.ac.cn
Prof. Dr. R. Krishna
Van't Hoff Institute for Molecular Sciences, University of Amsterdam
Science Park 904, 1098 XH Amsterdam (The Netherlands)
E-mail: R.Krishna@contact.uva.nl
Dr. L. Huang,[+] X. F. Yi, Prof. Dr. A. M. Zheng
State Key Laboratory of Magnetic Resonance and Atomic and Molecular Physics, National Center for Magnetic Resonance in Wuhan, Wuhan Institute of Physics and Mathematics, The Chinese Academy of Sciences
Wuhan 430071 (China)
E-mail: zhenganm@wipm.ac.cn
Prof. Dr. C. B. Fan,[+] S. Z. Pu
Jiangxi Key Laboratory of Organic Chemistry, Jiangxi Science and Technology Normal University
Nanchang 330013 (China)
E-mail: pushouzhi@tsinghua.org.cn
[+] These authors are co-first author.
Supporting information and the ORCID identification number(s) for the author(s) of this article can be found under: https://doi.org/10.1002/anie.201702484.

extensively explored in photochemistry and material science.[21] Notably, such isomerization usually results in significant difference in optical and electronic properties, leading to an important application as switching material, such as in fluorescent molecular, photochromic chiral, photocontrolled conductivity, and liquid-crystal switches.[22] Inspired by this, anchoring diarylethene in MOFs has been recently developed to give a CO_2 adsorption/release switch,[23] energy transfer switch,[24] and singlet oxygen switch in living cells.[25] However, the use of diarylethene to switch gas separation has not been reported. herein we aim to demonstrate that the use of photochromic diarylethene unit results not only in enhanced C_2H_2/C_2H_4 separation, but also photoswitching C_2H_2/C_2H_4 separation, leading to a significant application as a separation switch (Scheme 1).

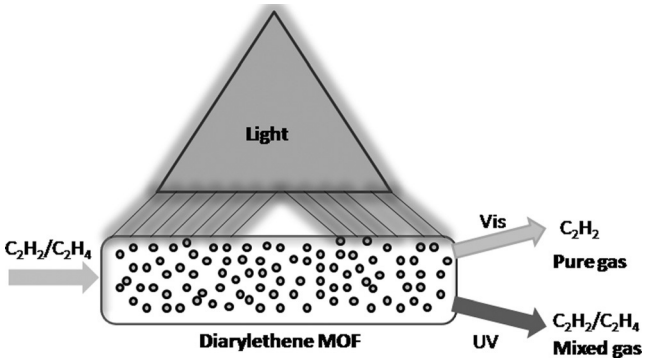

Scheme 1. Representation of a separation switch upon UV and visible light with a diarylethene MOF. Under UV irradiation, the diarylethene unit undergoes a ring-open to ring-closed transformation, leading to weak C_2H_2/C_2H_4 separation and thus generating mixed C_2H_2/C_2H_4 output. Visible irradiation induces recovery from the ring-closed form to ring-open form, resulting in high C_2H_2/C_2H_4 separation, generating pure C_2H_2 output.

The diarylethene MOF (**1**) was synthesized by using the previously reported method.[23] The resulted crystals determined at 293 K is consistent with the reported value and shown in Figure 1. As UV light cannot penetrate into the crystal samples, thereby the samples used in this work are treated by ball milling. The resulted bulk samples are confirmed by powder X-ray diffraction (Supporting Information, Figure S1), SEM (Supporting Information, Figure S2a), and laser particle size analyzer (Supporting Information, Figure S2b). It is clear that such mechanical operation does not affect the framework of **1**, and the size of the resulted particle is around one micrometer. The photochromic feature is confirmed by UV/Vis absorption spectra, where the absorption around 330 nm is characteristic of the π–π^* transitions of the diarylethene ligand in the ring-open conformation, and the new formed absorption around 630 nm implies the ring-open to ring-closed transformation (Supporting Information, Figure S3).[23]

Before carrying out gas adsorption, the activated samples of **1a** are prepared by a previously reported method.[23] Previous investigation suggests negligible N_2 adsorption but considerable CO_2 uptake. As shown in Figure 1 b,c, the C_2H_2 adsorption capacity of **1a** at 100 kPa and 293 K is 36.1 $cm^3 g^{-1}$,

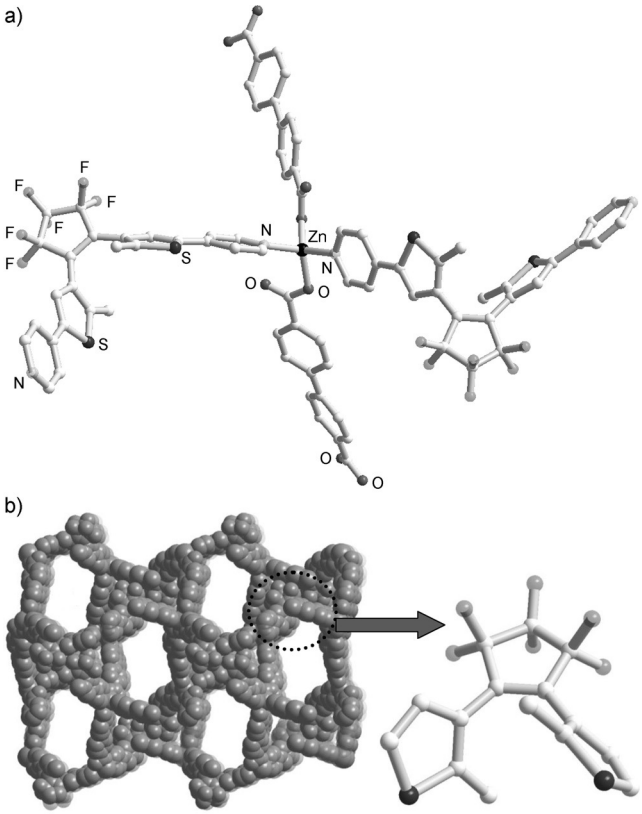

Figure 1. The structure of **1**. a) The coordination surrounding and the ligands in **1**; b) the 3D framework of **1**. All hydrogen atoms are omitted for clarity.

equal to 1.3 times larger than the corresponding C_2H_4 uptake of 27.4 $cm^3 g^{-1}$, suggesting preferential adsorption of C_2H_2 in **1a**. Note that at 100 kPa and 195 K the C_2H_2 uptake largely increases to be 120.3 $cm^3 g^{-1}$, almost 1.85 times bigger than corresponding value of 64.9 $cm^3 g^{-1}$ for C_2H_4 (Figure 2 a). The results imply that at low temperature more preferential adsorption of C_2H_2 over C_2H_4 is observed for **1a**. Most importantly, the C_2H_2 adsorption isotherm at 195 K (Supporting Information, Figure S4), unlike the C_2H_4 case, shows an abrupt increase in adsorption at a pressure of 2.0 kPa, indicative of a typical gate opening behavior under a gate opening pressure (P_{go}).[14] Below $P_{go} = 2.0$ kPa the uptake of C_2H_2 is less than 19.6 $cm^3 g^{-1}$, and after P_{go} the uptake of C_2H_2 sharply increases to 78.3 $cm^3 g^{-1}$, at 10 kPa. By contrast, gradual increase without clear abrupt increase is observed for C_2H_4 uptake, and a gradient change at 10 kPa is, as observed in some MOFs,[8c,13] due to a host–guest interaction between the MOF framework and C_2H_4 molecules. Such gate opening behavior is absolutely distinct with some reported flexible MOFs such as $Zn_2(bpdc)_2(bpee)$ (bpdc = 4,4′-biphenyldicarboxylate; bpee = 1,2- bipyriylethylene) in which gate opening effect is observed for both C_2H_2 and C_2H_4.[26] However, this behavior is similar to the results reported by Kitagawa in a 0-D framework[14] where C_2H_2, rather than CO_2, is observed to show a gate opening pressure. Note that our case is also different from the report by Kitagawa in that in the reported case gate opening effect leads to the sharp decrease in C_2H_2 uptake and consequently high CO_2/C_2H_2 selectivity (13 at

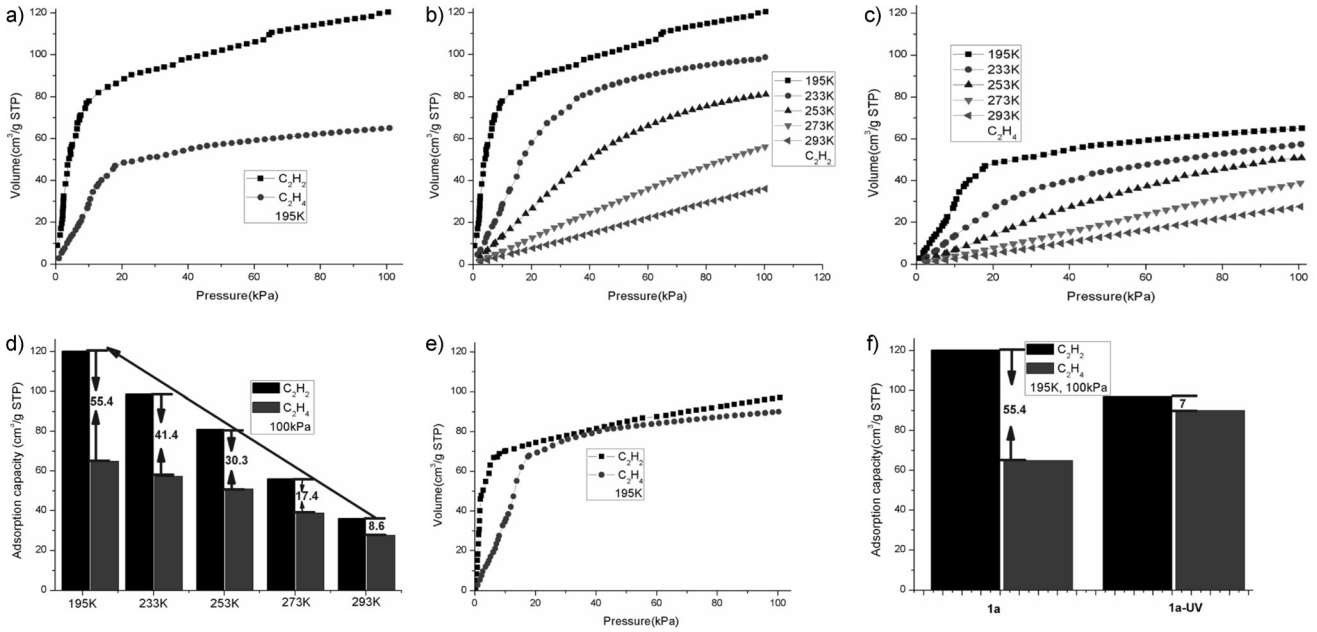

Figure 2. The C_2H_2 and C_2H_4 adsorption performance of **1a** (at various temperatures) and **1a**-UV. a) The adsorption isotherms of **1a** for C_2H_2 and C_2H_4 at 195 K. b) The adsorption isotherms of **1a** for C_2H_2 at various temperatures. c) The adsorption isotherms of **1a** for C_2H_4 at various temperatures. d) The difference in adsorption capacity of C_2H_2 and C_2H_4 at 100 kPa and various temperatures for **1a**. e) The adsorption isotherms of **1a**-UV for C_2H_2 and C_2H_4 at 195 K. f) The difference in adsorption capacity of C_2H_2 and C_2H_4 at 100 kPa and 195 K for **1a** and **1a**-UV.

273 K and 100 kPa), where in our case such effect enhances a sharp increase in C_2H_2 uptake and thus C_2H_2/C_2H_4 selectivity (47.1 at 195 K and 100 kPa).

As discussed above, **1a** undergoes the gate opening effect at 195 K, rather than 293 K, suggesting a temperature-dependent adsorption behavior. To further demonstrate such temperature dependency, additional adsorption experiments at 273, 253, and 233 K were conducted. As shown in Figure 2b–d, the C_2H_2/C_2H_4 uptake ratio for each temperature gives the hierarchy of 1.85@195 K > 1.72@233 K > 1.60@253 K > 1.45@273 K > 1.30@293 K, implying that **1a** shows significant temperature-dependent guest discriminatory gate effect.

To establish the mechanism for such uncommon phenomenon observed herein, we first test the flexibility of framework. The unit cell of **1a** for the same crystal is determined at various temperatures. No obvious alteration is seen in the unit cell (Supporting Information, Figure S5), relative to **1**, excluding any temperature-induced framework movement and suggesting rigid framework of **1a**. Most importantly, after UV (365 nm, namely **1a**-UV) irradiation compound **1a** no longer shows such guest discriminatory gate effect clearly, as seen by the comparable uptake of both C_2H_2 and C_2H_4 at 195 K (Figures 2d,e) and the absence of abrupt increase plus distinct adsorption isotherms for C_2H_2 adsorption at low pressure (Supporting Information, Figure S6). The observation of abnormality in the C_2H_2 and C_2H_4 adsorption among the adsorption capacity of 40–50 $cm^3 g^{-1}$ is due to the incomplete transformation of diarylethene unit and/or host–guest interactions between MOF framework and guest molecules. The ratio of C_2H_2/C_2H_4 uptake is largely reduced to be 1.08, which is far less than corresponding value of 1.85 for **1a**. It is believed that UV irradiation just induces a ring-open to ring-closed transformation of diarylethene ligand in **1a**. Accordingly, the results agree that such gate opening effect is directly related to the diarylethene unit. To exclude that this is resulted from a framework alteration between **1a** and **1a**-UV, in situ PXRD is tested (Supporting Information, Figure S7), where no additional and shifted Bragg peak, relative to that in **1a**, is observed in **1a**-UV, but significant enhancement of (002) intensity is observed for **1a**-UV, which is mainly due to a formation of a dense structure from a ring-open-to-ring-closed transformation of diarylethene ligand. Note that under irradiation by visible light, the PXRD patterns are fully recovered, which is comparable with that in **1a**, indicative of highly reversible transformation between **1a** and **1a**-UV.

To further elucidate the mechanism for such a guest discriminatory gate effect, we performed a density functional theory (DFT) calculations. Both C_2H_2 and C_2H_4 can be incarcerated by diarylethene unit (Figure 3). In the DFT-optimized guest-loaded structure, each diarylethene unit can incarcerate one C_2H_2 or C_2H_4 molecule via host–guest supramolecular interactions with the closest C–H···C distance of 3.48 Å for C_2H_2 and 3.56 Å for C_2H_4 between guest molecules and thiophene rings. Compared with the structure of diarylethene unit in **1a**, C_2H_2-loaded structure (Figure 3b) displays significant change in the diarylethene unit with a distance of 4.74 Å for two specific thiophene carbon atoms that connect to a methyl carbon, which is 1.29 times larger than that observed in **1a** (3.67 Å). A larger alteration in the diarylethene unit is needed in the C_2H_4-loaded structure (Figure 3c) with a corresponding distance of 4.86 Å, equal to 1.32 times larger than that in **1a**. Furthermore, we also note that except for the opening movement in the diarylethene unit the whole diarylethene ligand is maintained, as evidenced by

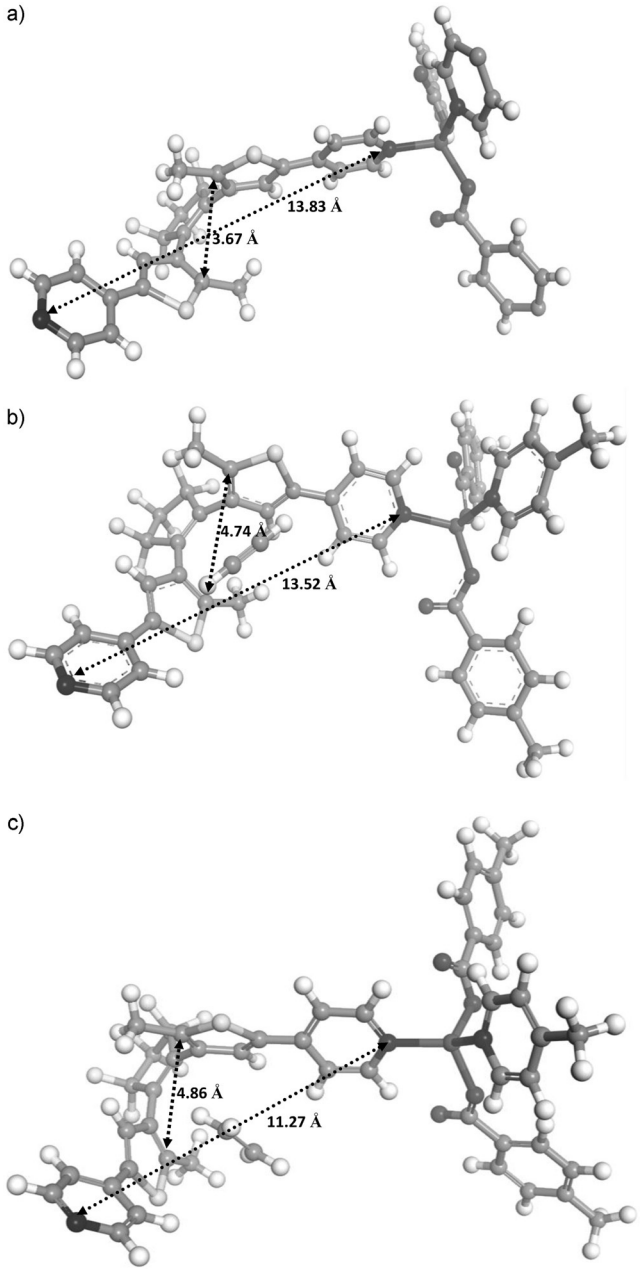

Figure 3. A comparison of diarylethene ligand among a) **1a**, b) C_2H_2-loaded structure, and c) C_2H_4-loaded structure. ⋆ The special thiophene carbon atom in the diarylethene ligand. The arrow indicates the distance between two special thiophene carbon atoms or the span between two pyridine nitrogen atoms of the diarylethene ligand.

the comparable distance for two pyridine nitrogen atoms of the diarylethene ligand between **1a** (13.83 Å) and C_2H_2-loaded structure (13.52 Å). The results agree that local opening in the diarylethene unit, rather than overall alteration within the MOF skeleton, could enable additional adsorption of C_2H_2, which is consistent with the experimental results. However, by contrast, C_2H_4-loaded structure gives a distance of 11.27 Å, implying a 2.56 Å compression for the whole diarylethene ligand, relative to that in **1a**. The results mean that, for C_2H_4, to occur such incarcerated phenomenon within diarylethene unit as observed for C_2H_2, **1a** needs undergo not only local movement of diarylethene unit but also intense alteration in the whole diarylethene ligand. However, such intense alteration in the whole diarylethene ligand is fully rejected by the rigid nature of MOF framework, consequently resulting in the incarceration of C_2H_4 in diarylethene unit within **1a** to give additional adsorption, as observed for C_2H_2, being completely blocked. In this regard, the observation of comparable adsorption of C_2H_2 and C_2H_4 in **1a**-UV is reasonable, owing to a ring-open to ring-closed transformation of the diarylethene unit that inherently refuses the incarceration phenomenon as observed in **1a**.

Furthermore, preferential adsorption of C_2H_2 over C_2H_4 in **1a** is also reflected in the data of isosteric heat of adsorption (Q_{st}). The calculation of binding energy of C_2H_2 and C_2H_4 based on the use of the Clausius–Clapeyron equation[27] is used to represent the isosteric heat of adsorption. The Q_{st} of C_2H_2 is approximately 17 kJ mol^{-1}, which is larger than the corresponding value of 11.5 kJ mol^{-1} for C_2H_4, indicative of stronger host–guest interactions for C_2H_2 over C_2H_4 (Figure 4a).

To establish the feasibility of C_2H_2/C_2H_4 separation, we first performed ideal adsorbed solution theory (IAST) calculations for adsorption selectivity,[28] and the results at 195, 273, and 293 K for materials of **1a** and **1a**-UV are shown in Figure 4b. Particularly remarkable is the ultrahigh C_2H_2/C_2H_4 selectivity of 47.1 at 195 K and 100 kPa, even superior to the recorded value of 44.8 by Chen et al. in SIFSIX-2-Cu-I,[15] suggesting its promising potential in C_2H_2/C_2H_4 at low temperature. However, with increase of temperature the selectivity is largely reduced with 3.2 at 273 K and 2.2 at 293 K, respectively. Such a 21.4-fold reduction in C_2H_2/C_2H_4 selectivity suggests highly temperature-dependent C_2H_2/C_2H_4 separation in **1a**, which is viable of the application as temperature-response C_2H_2/C_2H_4 separation switch. On the other hand, light as an easy-to-obtain source is also facile to control the C_2H_2/C_2H_4 adsorption selectivity. The samples after UV irradiation, **1a**-UV, only give a selectivity of 3.0 at 195 K and 100 kPa (Figure 4b), resulting in a 15.7-fold alteration relative to the value in **1a**, leading to a potential as light-response C_2H_2/C_2H_4 separation switch.

The performance of industrial fixed-bed adsorbers is dictated by a combination of adsorption selectivity and uptake capacity. To further evaluate the temperature- and light-dependent gas separation of **1a**, we performed transient breakthrough simulations using the simulation method described before.[11,14,15] Figure 4c presents the data on simulated transient breakthrough of C_2H_2/C_2H_4 mixture containing 50% C_2H_2 mixture in an adsorber bed packed with **1a** at various temperatures and **1a**-UV. The transient breakthrough simulation results are presented in terms of a dimensionless time τ (x-axis). The y-axis is the dimensionless concentrations at the outlet of the adsorber, normalized with respect to the inlet feed concentrations. As C_2H_4 could not be incarcerated in diarylethene unit, within adsorber bed of **1a** at 195 K it breaks through firstly with $\tau = 417$ and τ for C_2H_2 to breaks through is 1030, suggesting a 2.47 times longer breakthrough times within the adsorber bed for C_2H_2. By contrast, with the increasing temperature the ratio of breakthrough time for C_2H_2/C_2H_4 is largely reduced in the order 1.84@233 K >

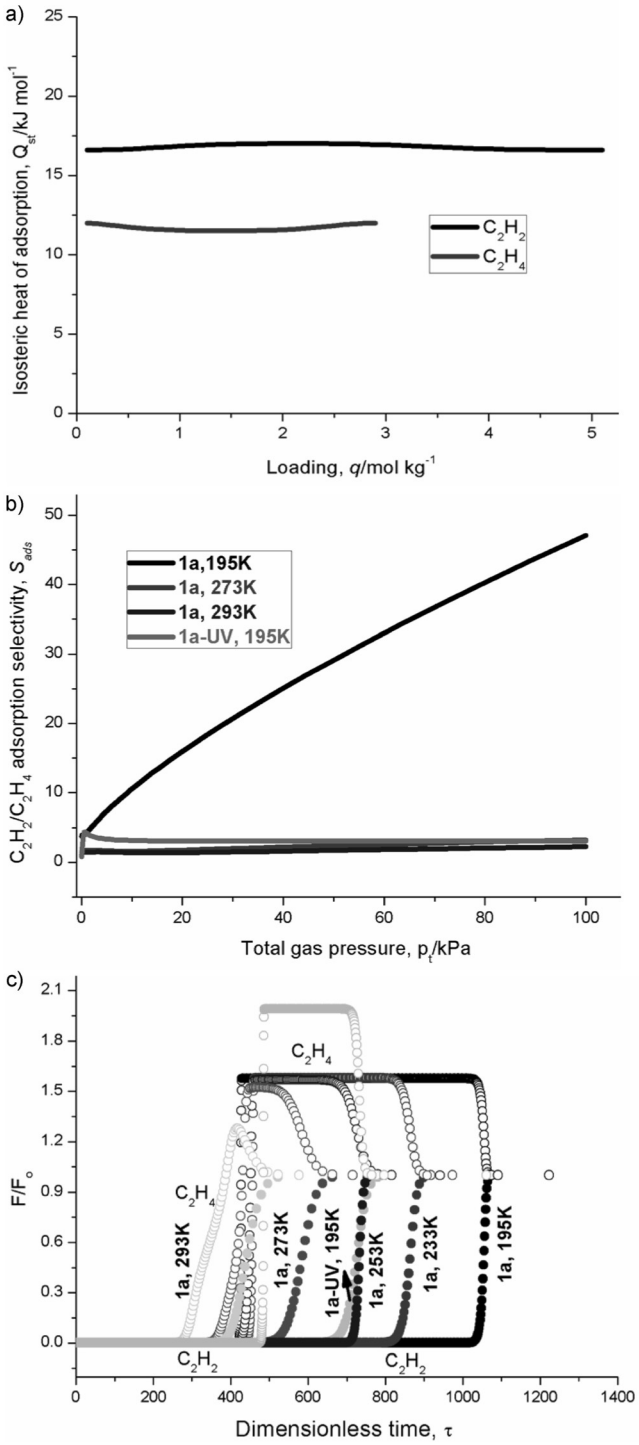

Figure 4. a) The isosteric heat of adsorption for C_2H_2 and C_2H_4 in **1a**. b) IAST calculations of 50/50 C_2H_2/C_2H_4 adsorption selectivity of **1a** at 195 K, 273 K, 293 K, and **1a**-UV at 195 K. c) Simulated transient breakthrough of C_2H_2/C_2H_4 mixture containing 50% C_2H_2 mixture in an adsorber bed packed with **1a** or **1a**-UV. The bulk gas phase is at set temperature and 20 kPa total pressure. The partial pressures of C_2H_2 and C_2H_4 in the inlet feed gas mixture are, respectively, $p_1 = 10$ kPa, $p_2 = 10$ kPa.

1.54@253 K > 1.42@273 K > 1.36@293 K, and the relative breakthrough time ($\Delta\tau$), defined by the difference of τ value between C_2H_2 and C_2H_4, sharply decreases from $\Delta\tau = 613$ at 195 K to $\Delta\tau = 99$ at 293 K, suggesting strong temperature-dependent separation. Alternatively, owing to the removal of additional adsorption for C_2H_2 from diarylethene unit, light facilitates to switch the C_2H_2/C_2H_4 separation, as attested by just 1.48 times longer reservation time within the adsorber bed of **1a**-UV for C_2H_2 than C_2H_4 and a largely reduced relative reservation time of $\Delta\tau = 225$.

Note that for such an application of light-responsive C_2H_2/C_2H_4 separation switch, acquiring its conversion ratio of diarylethene unit between the open- and closed-ring isomers is highly important, and thus we carried out the test of the ^{13}C MAS NMR spectra. As shown in the Supporting Information, Figure S8a, the as-synthesized samples do not show typical signal of the closed-ring form at 67 ppm, suggesting 100% open-ring form of diarylethene unit. However, for the samples after UV irradiation for 10 min, not only a new peak at 67 ppm, typical for the closed-ring form, appeared, but also an intensity-decreased peak at 120 ppm, typical for the open-ring form, were observed. This strongly suggests an incomplete ring-open to ring-closed transformation and coexistence of ring-closed and ring-open forms in the resulted samples (Supporting Information, Figure S8b). Accordingly a 61% conversion of diarylethene unit from ring-open isomer to ring-closed isomer is estimated. These results are consistent with the UV/Vis absorption spectra. Notably, 100% recovery from the ring-closed form to ring-open form can be obtained if visible irradiation (650 nm) is used on the colored samples (UV irradiation) for 30 min, as seen by the disappearance of the peak at 67 ppm and intensity-increased peak at 120 ppm (Supporting Information, Figure S8c). Furthermore, some previous reports have revealed that temperature has little effect on the ring-open to ring-closed transformation of diarylethene unit, whereas the inverse ring-closed-to-ring-open transformation is highly temperature-dependent; especially at low temperature, this is almost prohibited.[29] In this regard, we tested such a temperature-dependent photochromic property. As observed in reported cases,[29] the ring-open to ring-closed transformation of diarylethene unit is not temperature-dependent, since even at 77 K a single crystal of **1** under UV irradiation underwent smart photochromic reaction, consequently leading to the color change from yellow to blue. By contrast, inverse photochromic reaction under visible irradiation is stopped at such low temperature, because there is no detectable color change, but can be activated at a higher temperature such as 139 K, leading to the recovery of color change from blue to yellow. This is further confirmed by UV/Vis absorption spectra (Supporting Information, Figure S10), where the absorption around 630 nm, typical for ring-closed form, disappeared for the colored samples after visible irradiation (10 min) at 139 K.

In conclusion, we have demonstrated the first use of diarylethene MOF to separate C_2H_2/C_2H_4 mixture. Owing to a unique recognition to C_2H_2 within the diarylethene unit, a ultrahigh adsorption selectivity of C_2H_2 over C_2H_4 with the value of 47.1 is achieved at 195 K. Our investigation shows that such separation is very sensitive to temperature and light, leading to a significant switching effect and thus capability of using it as a temperature- and light-responsive C_2H_2/C_2H_4 separation switch.

Acknowledgements

This work was supported by the NSF of China (21661001, 21661002, 51373072, 21363009), the Natural Science Foundationof Jiangxi Province of China (20143ACB20002, 20151BAB203001), and the Young scientist training program of Jiangxi Province of China (20142BCB23018).

Conflict of interest

The authors declare no conflict of interest.

Keywords: gas separation · metal–organic frameworks · molecular switches · photochromism · selectivity

How to cite: *Angew. Chem. Int. Ed.* **2017**, *56*, 7900–7906
Angew. Chem. **2017**, *129*, 8008–8014

[1] a) H. Furukawa, K. E. Cordova, M. O'Keeffe, O. M. Yaghi, *Science* **2013**, *341*, 1230444; b) Y. J. Cui, B. Li, H. J. He, W. Zhou, B. L. Chen, G. D. Qian, *Acc. Chem. Res.* **2016**, *49*, 483; c) C. R. Kim, T. Uemura, S. Kitagawa, *Chem. Soc. Rev.* **2016**, *45*, 3828; d) B. Y. Li, M. Chrzanowski, Y. M. Zhang, S. Q. Ma, *Coord. Chem. Rev.* **2016**, *307*, 106; e) H. C. Zhou, J. R. Long, O. M. Yaghi, *Chem. Rev.* **2012**, *112*, 673; f) H. C. Zhou, S. Kitagawa, *Chem. Soc. Rev.* **2014**, *43*, 5415.

[2] a) P. Q. Liao, H. Y. Chen, D. D. Zhou, S. Y. Liu, C. T. He, Z. B. Rui, H. B. Ji, J. P. Zhang, X. M. Chen, *Energy Environ. Sci.* **2015**, *8*, 1011; b) Q. P. Lin, X. H. Bu, A. Kong, C. Y. Mao, X. Zhao, F. Bu, P. Y. Feng, *J. Am. Chem. Soc.* **2015**, *137*, 2235; c) S. Y. Zhang, L. Wojtas, M. J. Zaworotko, *J. Am. Chem. Soc.* **2015**, *137*, 12045; d) C. Liu, T. Y. Luo, E. S. Feura, C. Zhang, N. L. Rosi, *J. Am. Chem. Soc.* **2015**, *137*, 10508.

[3] a) A. J. Howarth, M. J. Katz, T. C. Wang, A. E. Platero-Prats, K. W. Chapman, J. T. Hupp, O. K. Farha, *J. Am. Chem. Soc.* **2015**, *137*, 7488; b) D. X. Xue, Y. Belmabkhout, O. Shekhah, H. Jiang, K. Adil, A. J. Cairns, M. Eddaoudi, *J. Am. Chem. Soc.* **2015**, *137*, 5034; c) Z. G. Gu, C. H. Zhan, J. Zhang, X. H. Bu, *Chem. Soc. Rev.* **2016**, *45*, 3122; d) J. P. Pang, F. L. Jiang, M. Y. Wu, C. P. Liu, K. Z. Su, W. G. Lu, D. Q. Yuan, M. C. Hong, *Nat. Commun.* **2015**, *6*, 7575.

[4] a) M. Yoon, R. Srirambalaji, K. Kim, *Chem. Rev.* **2012**, *112*, 1196; b) J. Liu, L. Chen, H. Cui, J. Zhang, L. Zhang, C. Y. Su, *Chem. Soc. Rev.* **2014**, *43*, 6011; c) O. R. Evans, W. Lin, *Acc. Chem. Res.* **2002**, *35*, 511; d) C. Wang, T. Zhang, W. Lin, *Chem. Rev.* **2012**, *112*, 1084; e) C. He, D. Liu, W. Lin, *Chem. Rev.* **2015**, *115*, 11079.

[5] a) A. M. Fracaroli, P. Siman, D. A. Nagib, M. Suzuki, H. Furukawa, F. D. Toste, O. M. Yaghi, *J. Am. Chem. Soc.* **2016**, *138*, 8352; b) K. Manna, P. F. Ji, F. X. Greene, W. B. Lin, *J. Am. Chem. Soc.* **2016**, *138*, 7488; c) Q. H. Yang, Q. Xu, S. H. Yu, H. L. Jiang, *Angew. Chem. Int. Ed.* **2016**, *55*, 3685; *Angew. Chem.* **2016**, *128*, 3749; d) H. L. Jiang, B. Liu, T. Akita, M. Haruta, H. Sakurai, Q. Xu, *J. Am. Chem. Soc.* **2009**, *131*, 11302; e) H. R. Moon, D. W. Lim, M. P. Suh, *Chem. Soc. Rev.* **2013**, *42*, 1807; f) X. H. Liu, J. G. Ma, Z. Niu, G. M. Yang, P. Cheng, *Angew. Chem. Int. Ed.* **2015**, *54*, 988; *Angew. Chem.* **2015**, *127*, 1002; g) Z. Chang, D. H. Yang, J. Xu, T. L. Hu, X. H. Bu, *Adv. Mater.* **2015**, *27*, 5432.

[6] a) B. Li, H. M. Wen, W. Zhou, J. Q. Xu, B. L. Chen, *Chem* **2016**, *1*, 557; b) B. Li, H. M. Wen, Y. J. Cui, W. Zhou, G. D. Qian, B. L. Chen, *Adv. Mater.* **2016**, *28*, 8819.

[7] a) K. J. Chen, D. G. Madden, T. Pham, K. A. Forrest, A. Kumar, Q. Y. Yang, W. I. Xue, B. Space, J. J. Perry IV, J. P. Zhang, X. M. Chen, M. J. Zaworotko, *Angew. Chem. Int. Ed.* **2016**, *55*, 10268; *Angew. Chem.* **2016**, *128*, 10424; b) P. Q. Liao, W. X. Zhang, J. P. Zhang, X. M. Chen, *Nat. Commun.* **2015**, *6*, 8697.

[8] a) Z. J. Zhang, S. C. Xiang, B. L. Chen, *CrystEngComm* **2011**, *13*, 5983; b) T. L. Hu, H. L. Wang, B. Li, R. Krishna, H. Wu, W. Zhou, Y. F. Zhao, Y. Han, X. Wang, W. D. Zhu, Z. Z. Yao, S. C. Xiang, B. L. Chen, *Nat. Commun.* **2015**, *6*, 7328; c) S. C. Xiang, Z. J. Zhang, C. G. Zhao, K. L. Hong, X. B. Zhao, D. R. Ding, M. H. Xie, C. D. Wu, M. C. Das, R. Gill, K. M. Thomas, B. L. Chen, *Nat. Commun.* **2011**, *2*, 204.

[9] a) Y. He, S. Xiang, Z. Zhang, S. Xiong, F. R. Fronczek, R. Krishna, M. O'Keeffe, B. Chen, *Chem. Commun.* **2012**, *48*, 10856; b) H. Xu, Y. He, Z. Zhang, S. Xiang, J. Cai, Y. Cui, Y. Yang, G. Qian, B. Chen, *J. Mater. Chem. A* **2013**, *1*, 77.

[10] S. R. Caskey, A. G. Wong-Foy, A. J. Matzger, *J. Am. Chem. Soc.* **2008**, *130*, 10870.

[11] F. Luo, C. S. Yan, L. L. Dang, R. Krishna, W. Zhou, H. Wu, X. L. Dong, Y. Han, T. L. Hu, M. O'Keeffe, L. L. Wang, M. B. Luo, R. B. Lin, B. L. Chen, *J. Am. Chem. Soc.* **2016**, *138*, 5678.

[12] a) L. T. Du, Z. Y. Lu, K. Y. Zheng, J. Y. Wang, X. Zheng, Y. Pan, X. Z. You, J. F. Bai, *J. Am. Chem. Soc.* **2013**, *135*, 562; b) A. Schneemann, E. D. Bloch, S. Henke, P. L. Llewellyn, J. R. Long, R. A. Fischer, *Chem. Eur. J.* **2015**, *21*, 18764.

[13] R. Matsuda, R. Kitaura, S. Kitagawa, Y. Kubota, R. V. Belosludov, T. C. Kobayashi, H. Sakamoto, T. Chiba, M. Takata, Y. Kawazoe, Y. Mita, *Nature* **2005**, *436*, 238.

[14] M. L. Foo, R. Matsuda, Y. Hijikata, R. Krishna, H. Sato, S. Horike, A. Hori, J. G. Duan, Y. Sato, Y. Kubota, M. Takata, S. Kitagawa, *J. Am. Chem. Soc.* **2016**, *138*, 3022.

[15] X. L. Cui, K. J. Chen, H. B. Xing, Q. W. Yang, R. Krishna, Z. B. Bao, H. Wu, W. Zhou, X. L. Dong, Y. Han, B. Li, Q. L. Ren, M. J. Zaworotko, B. L. Chen, *Science* **2016**, *353*, 141.

[16] C. Serre, C. Mellot-Draznieks, S. Surblé, N. Audebrand, Y. Filinchuk, G. Férey, *Science* **2007**, *315*, 1828.

[17] S. Q. Ma, D. F. Sun, D. Q. Yuan, X. S. Wang, H. C. Zhou, *J. Am. Chem. Soc.* **2009**, *131*, 6445.

[18] M. T. Wharmby, S. Henke, T. D. Bennett, S. R. Bajpe, I. Schwedler, S. P. Thompson, F. Gozzo, P. Simoncic, C. Mellot-Draznieks, H. Z. Tao, Y. Z. Yue, A. K. Cheetham, *Angew. Chem. Int. Ed.* **2015**, *54*, 6447; *Angew. Chem.* **2015**, *127*, 6547.

[19] a) T. H. Noh, O. S. Jung, *Acc. Chem. Res.* **2016**, *49*, 1835; b) D. H. Qu, Q. C. Wang, Q. W. Zhang, X. Ma, H. Tian, *Chem. Rev.* **2015**, *115*, 7543; c) A. J. McConnell, C. S. Wood, P. P. Neelakandan, J. R. Nitschke, *Chem. Rev.* **2015**, *115*, 7729; d) C. L. Jones, A. J. Tansell, T. L. Easun, *J. Mater. Chem. A* **2016**, *4*, 6714; e) J. Park, D. Q. Yuan, K. T. Pham, J. R. Li, A. Yakovenko, H. C. Zhou, *J. Am. Chem. Soc.* **2012**, *134*, 99; f) N. Yanai, T. Uemura, M. Inoue, R. Matsuda, T. Fukushima, M. Tsujimoto, S. Isoda, S. Kitagawa, *J. Am. Chem. Soc.* **2012**, *134*, 4501.

[20] a) R. Lyndon, K. Konstas, B. P. Ladewig, P. D. Southon, C. J. Kepert, M. R. Hill, *Angew. Chem. Int. Ed.* **2013**, *52*, 3695; *Angew. Chem.* **2013**, *125*, 3783; b) H. A. Li, M. M. Sadiq, K. Suzuki, R. Ricco, C. Doblin, A. J. Hill, S. Lim, P. Falcaro, M. R. Hill, *Adv. Mater.* **2016**, *28*, 1839; c) H. Q. Li, M. R. Hill, C. Doblin, S. Lim, A. J. Hill, P. Falcaro, *Adv. Funct. Mater.* **2016**, *26*, 4815.

[21] a) M. Irie, T. Fukaminato, T. Sasaki, N. Tamai, T. Kawai, *Nature* **2002**, *420*, 759; b) K. Matsuda, M. Irie, *J. Am. Chem. Soc.* **2000**, *122*, 7195; c) K. Matsuda, M. Irie, *J. Am. Chem. Soc.* **2000**, *122*, 8309; d) K. Matsuda, M. Irie, *J. Am. Chem. Soc.* **2001**, *123*, 9896.

[22] a) T. Fukaminato, T. Sasaki, T. Kawai, N. Tamai, M. Irie, *J. Am. Chem. Soc.* **2004**, *126*, 14843; b) N. Tanifuji, M. Irie, K. Matsuda, *J. Am. Chem. Soc.* **2005**, *127*, 13344; c) S. Lim, J. Seo, S. Park, *J. Am. Chem. Soc.* **2006**, *128*, 14542.

[23] F. Luo, C. B. Fan, M. B. Luo, X. L. Wu, Y. Zhu, S. Z. Pu, W. Y. Xu, G. C. Guo, *Angew. Chem. Int. Ed.* **2014**, *53*, 9298; *Angew. Chem.* **2014**, *126*, 9452.

[24] D. E. Williams, J. A. Rietman, J. M. Maier, R. Tan, A. B. Greytak, M. D. Smith, J. A. Krause, N. B. Shustova, *J. Am. Chem. Soc.* **2014**, *136*, 11886.
[25] J. Park, Q. Jiang, D. W. Feng, H. C. Zhou, *Angew. Chem. Int. Ed.* **2016**, *55*, 7188; *Angew. Chem.* **2016**, *128*, 7304.
[26] N. Nijem, H. H. Wu, P. Canepa, A. Marti, K. J. Balkus, Jr., T. Thonhauser, J. Li, Y. J. Chabal, *J. Am. Chem. Soc.* **2012**, *134*, 15201.
[27] D. W. Breck, *Zeolite Molecular Sieves*, Wiley, New York, **1974**.
[28] a) A. L. Myers, J. M. Prausnitz, *AIChE J.* **1965**, *11*, 121; b) R. Krishna, J. R. Long, *J. Phys. Chem. C* **2011**, *115*, 12941; c) R. Krishna, *Microporous Mesoporous Mater.* **2014**, *185*, 30; d) R. Krishna, R. Baur, *Sep. Purif. Technol.* **2003**, *33*, 213.
[29] a) M. Irie, T. Fukaminato, K. Matsuda, S. Kobatake, *Chem. Rev.* **2014**, *114*, 12174; b) D. Dulić, T. Kudernac, A. Pužys, B. L. Feringa, B. J. van Wees, *Adv. Mater.* **2007**, *19*, 2898.

Manuscript received: March 8, 2017
Version of record online: April 24, 2017

Angewandte Chemie
Eine Zeitschrift der Gesellschaft Deutscher Chemiker

Supporting Information

Significant Enhancement of C_2H_2/C_2H_4 Separation by a Photochromic Diarylethene Unit: A Temperature- and Light-Responsive Separation Switch

Cong Bin Fan[+], Le Le Gong[+], Ling Huang[+], Feng Luo, Rajamani Krishna,* Xian Feng Yi, An Min Zheng,* Le Zhang, Shou Zhi Pu,* Xue Feng Feng, Ming Biao Luo, and Guo Cong Guo**

anie_201702484_sm_miscellaneous_information.pdf

Supporting information

Experiments.

Materials and Physical Measurements. All the reagents, except for the diarylethene ligand that is synthesized by reported method,[23] used in this work are purchased from Alfa without any purification. X-ray powder diffraction were collected by a Bruker AXSD8 Discover powder diffractometer at 40 kV, 40 mA for Cu Kα, (λ = 1.5406Å). The simulated powder patterns were calculated by Mercury 1.4. The purity of the bulk products were determined by comparison of the simulated and experimental PXRD patterns. In-situ PXRD is also performed for the same sample without any movement on Bruker AXSD8 Discover powder diffractometer equipped with an UV or Vis equipment to provide UV (365 nm) and visible light (650 nm).

The gas sorption isotherms were collected on a Belsorp-max. Ultrahigh-purity-grade (>99.999%) C_2H_2 and C_2H_4 gases were used in this adsorption measurement. To maintain the experimental temperatures liquid nitrogen (77 K), temperature-programmed liquid nitrogen/ acetone bath (195 K, 233K, 253K), ice water bath (273 K), and water bath (293 K) were used respectively.

The samples in this work are prepared by ball milling as follows. Single crystal samples (500 mg) were placed in a 500 mL stainless steel jar, along with thirty-five 20 mm diameter stainless steel balls. Then, they are ground for 30 min in a PM-2L mill (Shanghai Precision Instrument Co., Ltd.) at 10 Hz.

Before carrying out adsorption experiments, the samples of **1a** (150 mg) were immerged in CH_3OH for three days, then degassed automatically in Belsorp-max at 60℃ for 24 h to generate the activated samples of **1a**.

The adsorption data of **1a**-UV is obtained based on the samples **1a** after UV irradiation for 10 min.

The UV and Vis irradiation is carried out by MejiroGenossen MUV-165 (3.8 W/cm^2) and MVL-210 (3.5 W/cm^2) with 365 nm and 650 nm filters, respectively. The samples were directly exposed under UV and Vis light with a distance about 80 cm between the light source and samples.

DFT calculations. The structural optimization of **1a** was performed with DMol ab initio quantum chemistry software of Accelrys' materials studio. The calculations were performed with the DNP basis sets, double numerical basis sets supplemented by polarization

functions.The generalized gradient approximation (GGA) with the Perdew–Burke–Ernzerhof exchange-correlation functionwas adopted. SCF density convergence, optimization energy convergence and gradient convergence equal to 0.00001, 0.0001 and 0.02 a.u, respectively.

The calculations of guest-incarcerated configuration were carried out using the Gaussian 09 program package, where wb97xd method with 6–31G (d) as basis sets was used. During the calculation, the full relaxation of **1a** cluster involving diarylethene unit was performed, and gas molecule was fixed.

Fitting of pure component isotherms.

The pure component isotherm data for C_2H_2 and C_2H_4 in **1a** at various temperatures and **1a**-UV at 195 K were fitted with the dual-site Langmuir-Freundlich isotherm model

$$q = q_{A,sat}\frac{b_A p^{\nu A}}{1+b_A p^{\nu A}} + q_{B,sat}\frac{b_B p^{\nu B}}{1+b_B p^{\nu B}} \quad (1)$$

with T-dependent parameters b_A, and b_B

$$b_A = b_{A0}\exp\left(\frac{E_A}{RT}\right); \quad b_B = b_{B0}\exp\left(\frac{E_B}{RT}\right) \quad (2)$$

The fitted parameters are provided in Table 1, and Table 2.

Table 1. Dual-site Langmuir-Freundlich parameter fits for C_2H_2 and C_2H_4 in **1a**.

	Site A				Site B			
	$q_{A,sat}$ mol kg^{-1}	b_{A0} Pa$^{-\nu A}$	ν_A	E_A kJ mol^{-1}	$q_{B,sat}$ mol kg^{-1}	b_{B0} Pa^{-1}	ν_B	E_B kJ mol^{-1}
C_2H_2	1.4	6.54×10^{-25}	3.3	57.2	3.8	4.37×10^{-8}	1	16.6
C_2H_4	1.2	1.41×10^{-18}	2.9	32.6	1.8	4.2×10^{-7}	1	12

Table 2. Dual-site Langmuir-Freundlich parameter fits for C_2H_2 and C_2H_4 in **1a-UV**.

	Site A				Site B			
	$q_{A,sat}$ mol kg^{-1}	b_{A0}	ν_A	E_A kJ mol^{-1}	$q_{B,sat}$ mol kg^{-1}	b_{B0}	ν_B	E_B kJ mol^{-1}

		$Pa^{-\nu A}$				Pa^{-1}		
C_2H_2	2.2	1.78×10^{-23}	2.8	61	2.2	3.32×10^{-6}	1	8
C_2H_4	1.9	8.63×10^{-21}	3.2	36.7	2.4	7.51×10^{-7}	1	10.6

Isosteric heat of adsorption.

The binding energy of C_2H_2 and C_2H_4 is reflected in the isosteric heat of adsorption, Q_{st}, defined as

$$Q_{st} = RT^2\left(\frac{\partial \ln p}{\partial T}\right)_q \tag{3}$$

IAST calculations of adsorption selectivities.

We consider the separation of binary C_2H_2/C_2H_4 mixtures. The adsorption selectivity for C_2H_2/C_2H_4 separation is defined by

$$S_{ads} = \frac{q_1/q_2}{p_1/p_2} \tag{4}$$

q_1, and q_2 are the molar loadings in the adsorbed phase in equilibrium with the bulk gas phase with partial pressures p_1, and p_2.

Transient breakthrough of C_2H_2/C_2H_4 mixtures in fixed bed adsorbers.

For the breakthrough simulations, the following parameter values were used: length of packed bed, L = 0.3 m; voidage of packed bed, □ = 0.4; superficial gas velocity at inlet, u= 0.04 m/s.

The total bulk gas phase is at settemperature and 20 kPa. The partial pressures of C_2H_2, and C_2H_4 in the inlet feed gas mixture are, respectively, p_1 = 10 kPa, p_2 = 10 kPa.The transient breakthrough simulation results are presented in terms of a *dimensionless* time, □ , (x-axis), defined by dividing the actual time, t, by the characteristic time, $\frac{L\varepsilon}{u}$. The$y$-axis is the dimensionless concentrations at the outlet of the adsorber, normalized with respect to the inlet feed concentrations.

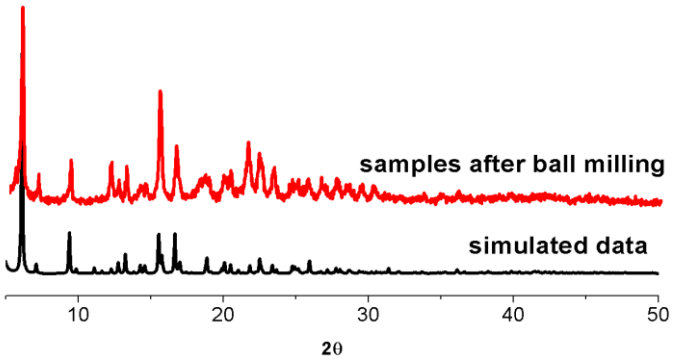

Figure S1. The PXRD patterns of samples after ball milling and the data simulated from the single crystal data.

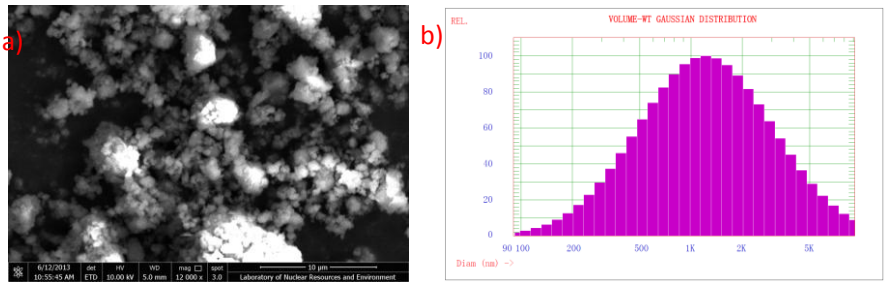

Figure S2. The morphology and size of particle of samples after ball milling.a) SEM image of samples after ball milling; b) size distributing of particle by laser particle size analyzer.

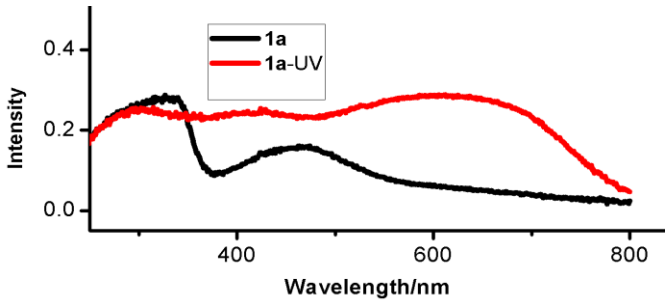

Figure S3. Absorption spectra of **1a** and **1a**-UVin the solid. **1a**-UV is obtained by UV irradiation on the samples **1a** for 10 min.

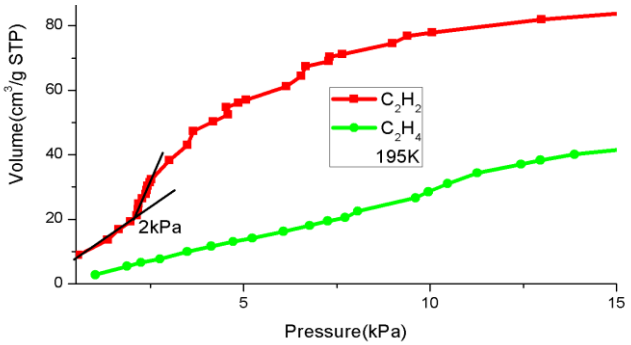

Figure S4. The C_2H_2 and C_2H_4 adsorption isotherms of **1a** at low pressure.

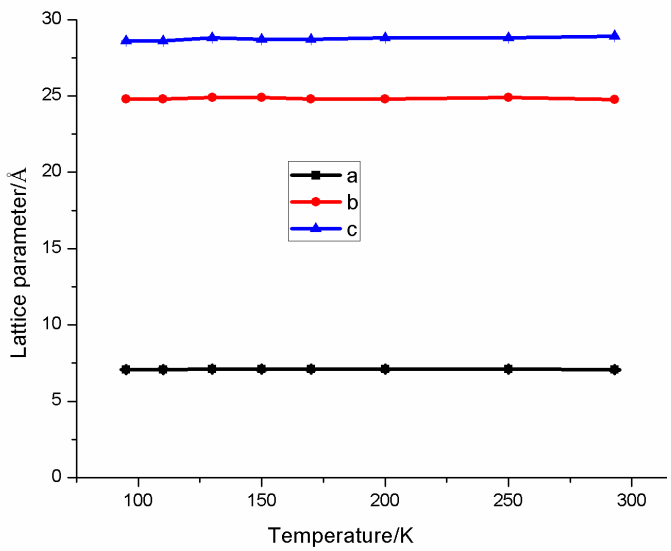

Figure S5. Crystal lattice parameter (*a*-, *b*, and *c*-axis length) of **1a** (crystal samples) determined at various temperatures.

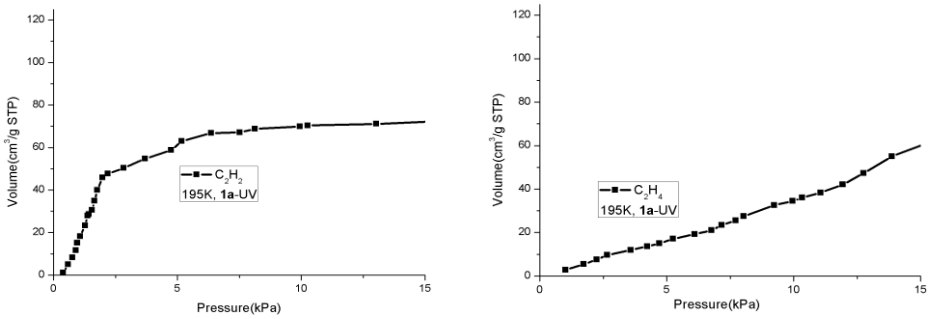

Figure S6. The C_2H_2 and C_2H_4 adsorption isotherms of **1a**-UVat low pressure.

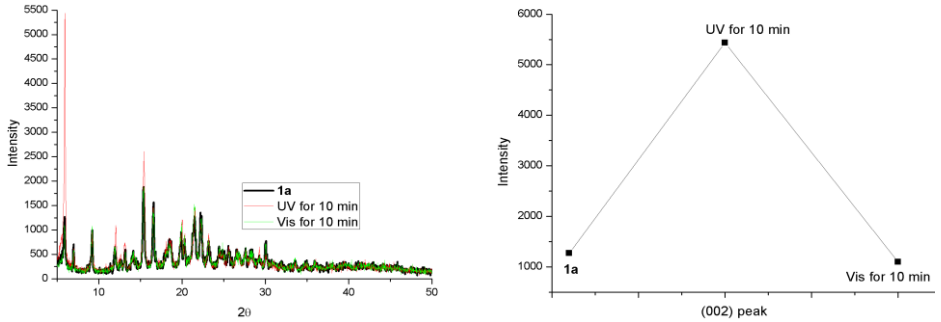

Figure S7. a)The in-situ PXRD patterns of **1a** under UV (365 nm, irradiation for 10 min) or visible light (650 nm, irradiation for 10 min). b) The change in intensity monitored by (002) peak for pristine **1a**, and it under UV irradiation for 10 min or visible light irradiation for 10 min.

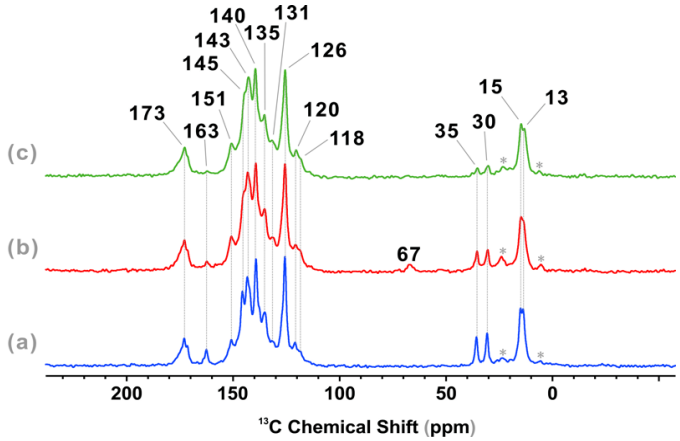

Figure S8. ^{13}C CP/MAS NMR spectra of **1**, **1a**-UV, and regenerated **1a**. The signal at 173 ppm is derived from carboxylate carbon atom. Signals among 151-126 ppm result from both carboxylate and diarylethene ligands. Signals around 120 ppm are ascribed to the thiophene carbons and carbons connecting to F atoms. Signal at 67 ppm is the carbon atoms connecting to CH_3 group for the samples after UV irradiation. Signals around 13 ppm are CH_3 group. Signals at 30 ppm, 35 ppm, and 163 ppm are the free DMF solvent molecule, where due to many times UV/Vis operation spontaneous loss of free DMF solvent molecule induces the gradual decrease of peak intensity.

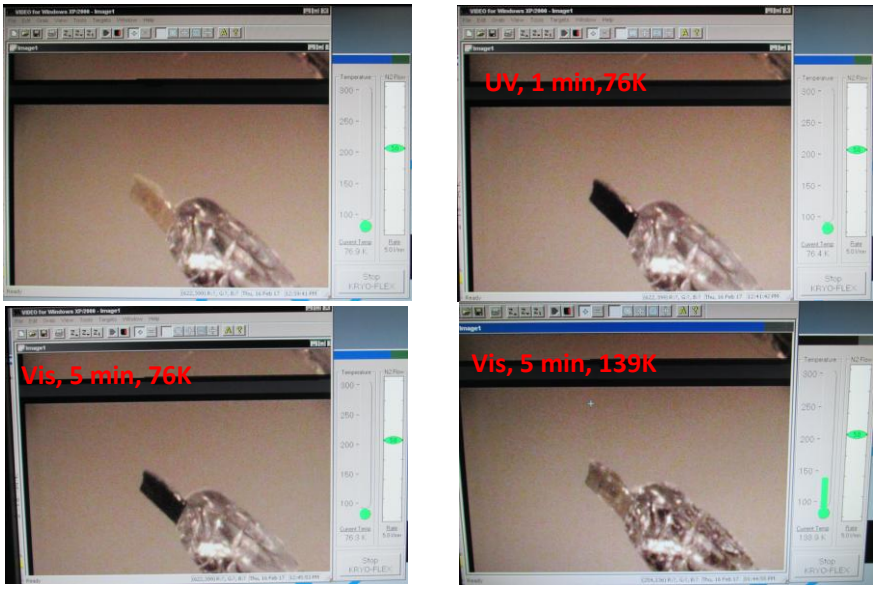

Figure S9. Photograph of crystal of **1** and it under UV or Vis irradiation at set temperature.

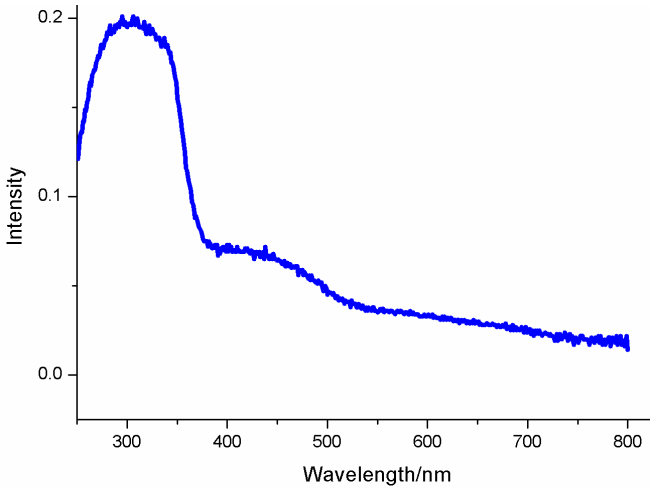

Figure S10. Absorption spectra of the solid samples, regenerated *via* Vis irradiation on the colored samples (UV irradiation for 1 min) for 10 min.